Interactions Remove the Quantization of the Chiral Photocurrent at Weyl Points

Alexander Avdoshkin,[1,*] Vladyslav Kozii,[1,2,*] and Joel E. Moore[1,2]
[1]Department of Physics, University of California, Berkeley, California 94720, USA
[2]Materials Sciences Division, Lawrence Berkeley National Laboratory, Berkeley, California 94720, USA

(Received 9 December 2019; accepted 29 April 2020; published 15 May 2020)

The chiral photocurrent or circular photogalvanic effect (CPGE) is a photocurrent that depends on the sense of circular polarization. In a disorder-free, noninteracting chiral Weyl semimetal, the magnitude of the effect is approximately quantized with a material-independent quantum e^3/h^2 for reasons of band topology. We study the first-order corrections due to the Coulomb and Hubbatrd interactions in a continuum model of a Weyl semimetal in which known corrections from other bands are absent. We find that the inclusion of interactions generically breaks the quantization. The corrections are similar but larger in magnitude than previously studied interaction corrections to the (nontopological) linear optical conductivity of graphene, and have a potentially observable frequency dependence. We conclude that, unlike the quantum Hall effect in gapped phases or the chiral anomaly in field theories, the quantization of the CPGE in Weyl semimetals is not protected but has perturbative corrections in interaction strength.

DOI: 10.1103/PhysRevLett.124.196603

The quantization of physical observables has become a cornerstone in condensed matter physics for the past few decades, guiding theoretical and experimental efforts across a wide range of fields. Starting from the discovery of quantum Hall effect, it led to multiple breakthroughs in our understanding of quantum systems. For example, identifying the quantization of Berry phase led to the discovery of topological insulators [1]. A few examples of quantization of electronic and optical properties have been identified in metallic systems as well, such as the universal optical conductivity and optical transmittance in graphene [2–5] and, more recently, the circular photogalvanic effect (CPGE) in Weyl semimetals [6] and crystals with multifold nodal fermions [7–10].

One of the crucial questions in the study of topological materials, from both experimental and theoretical perspectives, is whether the quantized features are robust against interactions and disorder. In most cases, weak interactions do not destroy or qualitatively change gapped topological phases [11]. In particular, the quantum Hall and quantum anomalous Hall conductivities are known to preserve the quantized value even in the presence of a weak interaction [12–18], which is intimately related to the topological nature of the effect [12,14,15] and ultimately its connection to adiabatic transport [19].

For Weyl fermions, the effect of interactions was exhaustively studied in the context of the chiral anomaly —nonconservation of the chiral charge without an explicit breaking of the chiral symmetry [20,21]. It has long been known that the anomaly is not renormalized by interactions that do not explicitly break the chiral symmetry [22,23]. Analogously to the quantum Hall effect, this nonrenormalizability is deeply rooted in the topological nature of the chiral anomaly [24–26]. The chiral anomaly, however, leads to quantization of the chiral current, which in condensed matter is not the observable electrical current but rather a pumping between Weyl nodes, and hence it has not yet been possible to observe the quantization despite various proposals [27,28].

In this Letter, we study the effect of electron-electron interactions on the CPGE, another quantized response in nodal semimetals [6]. The CPGE is the production of a dc current by a circularly polarized light incident on a surface of the material [29–35]. In particular, the CPGE is the part of photocurrent that switches sign depending on the sign of the light polarization. This is a nonlinear response, second order in electric field, and hence requires the breaking of inversion symmetry; such responses can have topological content [36]. In Weyl semimetals that are also free of mirror symmetries, the CPGE becomes approximately quantized over some range of frequencies. As found in Ref. [6], the intrinsic contribution from a single Weyl point to the CPGE, an injection current $\mathbf{j}$, is quantized and has the value

$$\frac{d\mathbf{j}}{dt} = \beta_0(\omega)\mathbf{E}_\omega \times \mathbf{E}_{-\omega}, \qquad \beta_0(\omega) = i\frac{\pi e^3}{3h^2}C, \tag{1}$$

where e is the electron charge, $h = 2\pi\hbar$ is the Planck's constant, and C is the topological charge of the node. The important prerequisite for this result is the absence of inversion and mirror symmetries. Then nodes of different chiralities are located at different energies. Consequently, for a certain frequency range, one node contributes exactly the quantized value (1) from the transitions across the Weyl point, while the second one does not have such interband transitions because of Pauli blocking. The intraband

contribution to the CPGE current originating, e.g., from the indirect disorder-assisted transitions and allowed even at low frequencies, is typically at least an order of magnitude smaller and governed by previous semiclassical calculations [32–35]. So while the CPGE involves generation of a three-dimensional current density from two powers of electromagnetic field, like the chiral anomaly, unlike the chiral anomaly it can be observed in the overall electrical current, not the chiral current between nodes. Remarkably, this effect was recently predicted [37], and the distinctive frequency dependence observed [38], in the chiral Weyl semimetal RhSi.

We show using a minimal continuum model of a chiral Weyl semimetal that generic interactions give corrections to the perfect quantization of the CPGE, in contrast to the chiral anomaly. This model has the feature that corrections from other pieces of the Fermi surface are absent and the CPGE is exactly quantized without interactions for a range of frequencies. Furthermore, as was shown in Ref. [6], the quantization within the noninteracting two-band model is quite robust in the sense that it does not depend on such material or model-specific details as the Fermi velocity, tilt of the node, or the exact position of the chemical potential, and is given by Eq. (1). While the topological charge of the nodes C, when properly defined, is not affected by weak interactions [39,40], we find that the universal proportionality between the CPGE coefficient β and the topological charge, Eq. (1), does not hold in the presence of interactions. Using the low-energy field theory suitable for Weyl fermions, we demonstrate that the CPGE response acquires a nonuniversal correction even at weak coupling, in the sense that this correction depends on such material-specific parameters as the Fermi velocity or dielectric constant [41]. So while e^3/h^2 remains the natural scale for the CPGE response, there are potentially observable interaction effects that need not be small in real materials. We use the Hubbard and screened Coulomb potentials as examples.

Our results imply that the CPGE is an example of a quantized response which is not protected by topology beyond the non-interacting limit, and hence gets renormalized by arbitrarily weak interactions. In some sense, this scenario is similar to the effect of the interaction corrections to the (nontopological) optical conductivity in graphene. While the non-interacting consideration leads to the quantized value $e^2/4\hbar$ [2–5], the presence of interactions is known to contribute additional nonuniversal correction [43–51]. Similar results have been recently obtained for the optical conductivity in nodal-line semimetals [52].

The calculation of the numerical coefficient for the interaction correction in graphene turned out to be a nontrivial task. Originally, three different values of this coefficient were obtained for the hard-cutoff, soft-cutoff, and dimensional regularization schemes [43–47], leading to an intensive discussion regarding the choice of the correct one. The reason for such a peculiar behavior is rooted in the ultraviolet anomaly [45]: when applied naïvely, different approaches differently account for the high-energy states, resulting in different answers. It was shown later that, when the renormalization procedure is performed carefully, the soft-cutoff and dimensional regularizations lead to the same answer [50,51]. We also encounter the same anomaly in our study. We find that the results obtained within the soft-cutoff and the dimensional regularization procedures agree with each other, while the scheme with the hard cutoff, which implies neglecting the electron states with momenta exceeding certain ultraviolet value, leads to a different answer. This is somewhat natural, since the presence of a hard cutoff violates the Ward-Takahashi identity and incorrectly accounts for the contribution from the high-energy states, leading to a result which is only qualitatively correct.

Quantization of the CPGE in the absence of interaction.—Before presenting the main results of our Letter, we first reproduce the result for the non-interacting problem [6] using the framework of Feynman diagrams. The detailed derivation of the second-order response within the Keldysh formalism is given in Ref. [53] (see also Refs. [54,55]). In this Letter, however, we find it more convenient to use the Matsubara imaginary time formalism [56], which is equivalent to the Keldysh approach.

We start with a noninteracting system of two identical Weyl nodes of opposite chirality separated by energy $|\mu_1| + |\mu_2|$, as shown in Fig. 1. We assume for definiteness that the chemical potential for the first node is negative, $\mu_1 < 0$, while for the second node it is positive, $\mu_2 > 0$. The low-energy Hamiltonian of the system then takes the form

$$H_0 = \sum_{\mathbf{k}} \psi^\dagger_{1\mathbf{k}} (v_F \mathbf{k}\cdot\boldsymbol{\sigma} - \mu_1)\psi_{1\mathbf{k}} + \psi^\dagger_{2\mathbf{k}} (-v_F \mathbf{k}\cdot\boldsymbol{\sigma} - \mu_2)\psi_{2\mathbf{k}}, \tag{2}$$

where ψ_1 and ψ_2 are two-component fermion spinors describing the states near the first and second node, respectively, $\boldsymbol{\sigma}$ is a vector of pseudospin Pauli matrices,

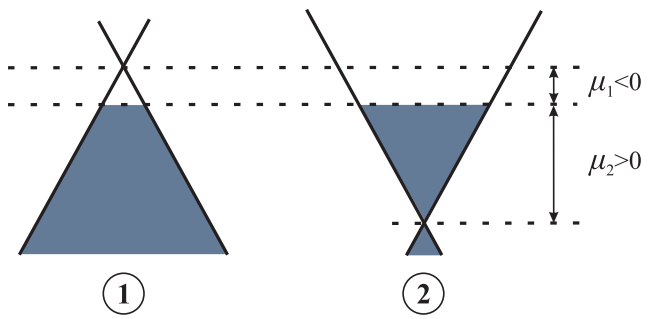

FIG. 1. Schematic picture of two Weyl nodes of opposite chirality separated by energy $|\mu_1| + |\mu_2|$. The quantization of the circular photogalvanic effect in the noninteracting material occurs provided $2|\mu_1| < \omega < 2|\mu_2|$.

and v_F is the Fermi velocity. Here and in what follows, we set $\hbar = 1$ for brevity, unless explicitly stated otherwise. The different sign of the Fermi velocities reflects the fact that the nodes have different chiralities.

We assume that the nodes are well separated in momentum space, and consequently the contribution to the (uniform) photocurrent can be calculated separately for each node. For definiteness, we focus on the first node for now. The expression for the second-order photocurrent reads as

$$j^\gamma(\Omega) = \frac{\chi^{\alpha\beta\gamma}(\omega_1,\omega_2) + \chi^{\beta\alpha\gamma}(\omega_2,\omega_1)}{\omega_1\omega_2} E^\alpha_{\omega_1} E^\beta_{\omega_2}, \quad (3)$$

where $\Omega \equiv \omega_1 + \omega_2$, and the factors $\omega_{1,2}$ in the denominator originate from the relation between the electric field and the vector potential $\mathbf{E}_\omega = i\omega\mathbf{A}_\omega$. The analytical expressions for the tensor $\chi(i\omega_1, i\omega_2)$ in Matsubara frequencies is given by [53]

$$\chi^{\alpha\beta\gamma}(i\omega_1, i\omega_2) = T\sum_{\varepsilon_n} \int \frac{d^3k}{(2\pi)^3} \mathrm{tr}[\hat{j}^\alpha G(i\varepsilon_n - i\omega_1, \mathbf{k}) \times \hat{j}^\beta G(i\varepsilon_n - i\Omega, \mathbf{k}) \hat{j}^\gamma G(i\varepsilon_n, \mathbf{k})], \quad (4)$$

with $\varepsilon_n = \pi T(2n+1)$ and T is temperature. The current operator in this expression equals

$$\hat{j}^\alpha = e\frac{\delta \hat{H}_0(\mathbf{k})}{\delta k^\alpha} = e v_F \sigma^\alpha, \quad (5)$$

while the Matsubara Green's function has the form

$$G(i\varepsilon_n, \mathbf{k}) = \frac{1}{2}\left[\frac{P_+(\mathbf{k})}{i\varepsilon_n - v_F k + \mu_1} + \frac{P_-(\mathbf{k})}{i\varepsilon_n + v_F k + \mu_1}\right], \quad (6)$$

and we introduced the projectors onto the conduction and the valence bands $P_\pm(\mathbf{k}) = I \pm \hat{\mathbf{k}}\cdot\boldsymbol{\sigma}$ with $\hat{\mathbf{k}} \equiv \mathbf{k}/k$. We emphasize again that we have only focused on the first node thus far; the contribution from the second node is obtained analogously.

Interestingly, the expression for $\chi(i\omega_1, i\omega_2)$ in the case of Weyl semimetals can be obtained exactly at $T = 0$. Delegating the details of the calculation to the Supplemental Material [57], we present the answer:

$$\chi^{\alpha\beta\gamma}(i\omega_1, i\omega_2) = \frac{e^3}{48\pi^2}\varepsilon^{\alpha\beta\gamma} \frac{\Omega^3(\omega_2-\omega_1)\ln(4\mu_1^2+\Omega^2) + \omega_1^3(\omega_2+\Omega)\ln(4\mu_1^2+\omega_1^2) - \omega_2^3(\omega_1+\Omega)\ln(4\mu_1^2+\omega_2^2)}{\omega_1\omega_2\Omega}, \quad (7)$$

where $\varepsilon^{\alpha\beta\gamma}$ is the fully antisymmetric Levi-Civita tensor. Equation (7), along with Eq. (3), is the first important result of our work, which describes the second-order response to external electric fields at arbitrary frequencies.

To obtain the injection current, we need to perform the analytic continuation to real frequencies, $i\omega_{1,2} \to \omega_{1,2} + i0$, and set $\omega_1 = \omega + \Omega$, $\omega_2 = -\omega$ with $\Omega \to 0$ [59]:

$$j^\gamma(\Omega) = -\frac{1}{12\pi}\frac{e^3}{\Omega}\varepsilon^{\alpha\beta\gamma}E^\alpha_\omega E^\beta_{-\omega}\Theta(\omega - 2|\mu_1|). \quad (8)$$

In the time domain, the $\Omega \to 0$ limit exactly corresponds to Eq. (1) with $C = 1$ and the CPGE coefficient given by

$$\beta_0 = i\frac{\pi e^3}{3h^2}\Theta(\omega - 2|\mu_1|). \quad (9)$$

Here we explicitly restored the Planck's constant $h = 2\pi\hbar$ for clarity.

The contribution from the second Weyl point has a similar form, but with the opposite sign due to different chirality, and μ_2 instead of μ_1 in the Heaviside step function. Consequently, in the frequency range $2|\mu_1| < \omega < 2|\mu_2|$, the CPGE in a noninteracting Weyl system becomes truly quantized and does not depend on the material-specific parameters such as the Fermi velocity, the exact position of the chemical potential, or the distance between the nodes, and is given by Eq. (1). As we show below, the perfect quantization breaks down in the presence of interactions.

Interaction corrections to the CPGE: the Hubbard potential.—Now we demonstrate by an explicit calculation that the electron-electron interactions destroy the quantization of the CPGE. As an example, we start with the Hubbard interaction and consider the static Coulomb potential later.

Generally (pseudospin conserving) electron-electron interaction is described by a Hamiltonian of the form

$$H_{\mathrm{int}} = \frac{1}{2}\sum_{i,j=1}^{2}\sum_{\mathbf{k},\mathbf{p},\mathbf{q}} \psi^\dagger_{\mathbf{k}-\mathbf{q},i,s}\psi_{\mathbf{k},i,s}\psi^\dagger_{\mathbf{p}+\mathbf{q},j,s'}\psi_{\mathbf{p},j,s'}V(\mathbf{q}) + \frac{1}{2}\sum_{i=1}^{2}\sum_{\mathbf{k},\mathbf{p},\mathbf{q}} \psi^\dagger_{\mathbf{k}-\mathbf{q},i,s}\psi_{\mathbf{k},\bar{i},s}\psi^\dagger_{\mathbf{p}+\mathbf{q},\bar{i},s'}\psi_{\mathbf{p},i,s'}V(\mathbf{K}_0). \quad (10)$$

We explicitly write down the summation over the nodal indices i, j, and the summation over the pseudospin indices s, s' is implied. Symbol $\bar{i}$ stands for the node different from node i and $\mathbf{K}_0$ is the distance between the nodes in the momentum space (we assume $K_0 \gg p, k, q$).

The first term in Eq. (10) stands for the intranodal scattering, while the second one describes the scattering

between the nodes, and we neglect processes that do not conserve the number of particles within each node separately (since they also violate momentum conversation).

To the first order in interaction, corrections to photocurrent are given by the self-energy and vertex corrections shown diagrammatically in Fig. 2. Solid and dashed lines correspond to the electron propagators of the first and the second nodes, respectively.

In the case of the Hubbard potential, $V(\mathbf{q}) = -\lambda$, the self-energy diagrams are just proportional to the total number of holes in the first node, N_h, or the number of electrons in the second node, N_e: $\Sigma^{(a)} = -\Sigma^{(c)}/2 = -\lambda N_h/2$, $\Sigma^{(b)} = -\Sigma^{(d)}/2 = \lambda N_e/2$. Taken together, these corrections only renormalize chemical potential, $\delta\mu = -\sum_i \Sigma^{(i)} = \lambda(N_e - N_h)/2$, which, in turn, shifts the range of frequencies where the CPGE is observed. This correction does not change the quantized value of the CPGE itself.

The vertex corrections, on the contrary, have a more profound effect and destroy the quantization of the CPGE. The correction to the CPGE coefficient β_0, Eq. (9), due to the intranodal interaction is given by Fig. 2(e) and equals [after the summation over all three current vertices in Eq. (4)]

$$\delta\beta^{(1)}(\omega) = -\beta_0 \frac{\lambda}{24\pi^2 v_F^3} \times \left(6v_F^2\Lambda^2 - 6\mu_1^2 - \omega^2 \ln\frac{|\omega^2 - 4\mu_1^2|}{4v_F^2\Lambda^2 - \omega^2}\right), \quad (11)$$

where Λ is the high-momentum ultraviolet (UV) cutoff.

The strong UV divergence of this result is cured once we take the internodal scattering into account. Indeed, the short-ranged nature of the Hubbard interaction allows for the corrections shown in Fig. 2(f), $\delta\beta^{(2)}(\omega)$, which contributes with the overall opposite sign due to the opposite chirality of the second node. Hence, after adding up both intra- and internodal contributions, we obtain the total correction to the CPGE coefficient (see the Supplemental Material [57] for details)

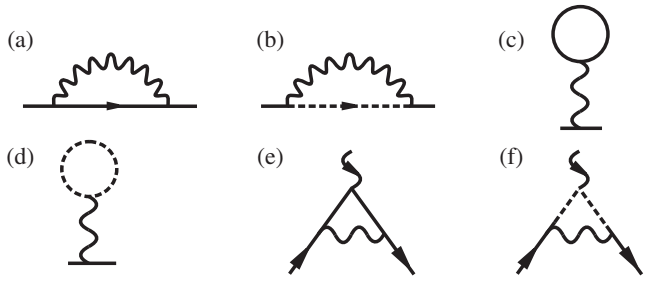

FIG. 2. First-order self-energy [(a)–(d)] and vertex [(e)–(f)] corrections. Solid and dashed lines correspond to the Green's function of the first and second node, respectively. Diagrams (a), (c), and (e) describe the intranodal processes, while (b), (d), and (f) stand for the internodal scattering (important only for the Hubbard interaction).

$$\delta\beta(\omega) = \delta\beta^{(1)}(\omega) + \delta\beta^{(2)}(\omega) = -\beta_0 \frac{\lambda}{24\pi^2 v_F^3}\left(6\mu_2^2 - 6\mu_1^2 - \omega^2 \ln\left|\frac{\omega^2 - 4\mu_1^2}{\omega^2 - 4\mu_2^2}\right|\right). \quad (12)$$

We see that the first-order interaction correction is free of the UV divergencies, but is nonzero and has a characteristic frequency dependence.

Interaction corrections to the CPGE: the Coulomb potential.—The whole analysis for the Coulomb potential is similar to that for the Hubbard interaction, with few important differences which we highlight below. The static screened Coulomb interaction that we focus on is given by Eq. (10) with

$$V(\mathbf{q}) = \frac{4\pi e^2}{\varepsilon_0(q^2 + q_0^2)}, \quad (13)$$

where e is the electron's charge, ε_0 is the dielectric constant due to core electrons, and q_0 is the Thomas-Fermi wave vector, respectively. The latter can be expressed through the fine-structure constant and the density of states at the Fermi level [60]. We, however, keep it an independent parameter for the purpose of generality, so that the interaction has the same form as the Yukawa potential.

Because of the long-ranged nature of the Coulomb interaction, one can focus on the correction due to the intranodal processes described by the first term in Eq. (10) only, while the contribution from the internodal scattering can be shown to be parametrically small. The correction is given by Figs. 2(a) and 2(e), and Fig. 2(c) describes the $q = 0$ component of the Coulomb interaction which is cancelled by the positive background. It can be straightforwardly shown that both the self-energy and vertex corrections to the CPGE coefficient β are logarithmically UV divergent, see the Supplemental Material [57]. The total answer, however, does not explicitly depend on the UV cutoff Λ and is given by

$$\delta\beta = \beta_0 \frac{e^2}{\pi v_F \varepsilon_0} F\left(\frac{v_F q_0}{\omega}, \frac{|\mu_1|}{\omega}\right). \quad (14)$$

The function $F(x, y)$ is a smooth function independent of Λ, which is shown in Fig. 3 and with the exact expression given in the Supplemental Material [57]. It turns out, however, that the particular form of $F(x, y)$ is sensitive to the regularization procedure. Thus, the answer obtained within the hard-cutoff (hc) regularization (which effectively cuts off the electron spectrum beyond the UV momentum scale Λ) is different from that obtained by the soft-cutoff (sc) and dimensional regularization (dr), and they all are related according to

$$F^{\mathrm{sc}}(x, y) = F^{\mathrm{dr}}(x, y) = F^{\mathrm{hc}}(x, y) - 1. \quad (15)$$

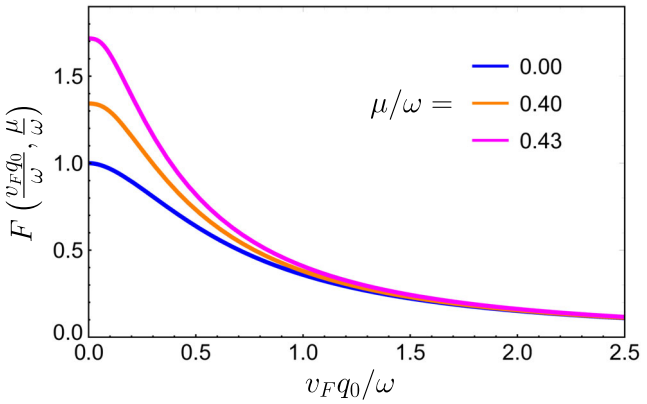

FIG. 3. The dependence of function F, Eq. (14), on q_0 at $|\mu|/\omega = 0.00$, 0.40, and 0.43 for the cases of the soft-cutoff and the dimensional regularizations. At $v_F q_0 \gg \omega$, all curves approach $F = 0$.

This peculiar result is similar to what happens with the interaction correction to the optical conductivity in graphene. The origin of the discrepancy is rooted in the way that different regularization procedures account for the high-energy (of order $v_F\Lambda$) states. The hard-cutoff scheme completely neglects the high-energy contribution and, as a result, violates the Ward-Takahashi identity. Hence the answer obtained within this procedure is only qualitatively correct.

The interaction corrections (12) and (14), along with the general response function for the noninteracting system (7), are the main calculational results of this work. In graphene, the interaction corrections seem experimentally to be small [5], but in the present case we expect the interaction corrections to be significant, unless the effective dielectric constant is rather large, and potentially observable.

Conclusions.—In conclusion, using the Hubbard and the static Coulomb interactions as examples, we have shown that the interactions destroy the quantization of the CPGE. We have found that, in case of the Coulomb interaction, the correction depends on the way one regularizes the contribution from the high-energy states, leading to the wrong result if the hard cutoff is used. This result is similar to that for the interaction correction to optical conductivity in graphene. Unlike graphene, however, where the quantization of optical conductivity even in a noninteracting system is not protected by topology, the quantization of the CPGE in noninteracting Weyl semimetals is tight to the monopole strength of the Weyl nodes. Hence, our result implies that, since the topological charge of the node remains unchanged, the interactions change the relation between the CPGE injection current and the nodal strength. It may be possible to observe the interaction effects on the frequency dependence of the plateau in the photocurrent, especially if the effects of disorder can be minimized by a short pulse or a difference-frequency-generation approach [61]. We expect the same qualitative results to hold for the higher-order nodal materials [10], though we leave an explicit calculation in this case for a future study.

We thank Fernando de Juan, Adolfo Grushin, and Daniel Parker for discussions and collaboration on related projects. We also appreciate comments from Jörg Schmalian, Inti Sodemann, and Igor Herbut. This work was supported by the Quantum Materials program at LBNL, funded by the US Department of Energy under Contract No. DE-AC02-05CH11231 (V. K. and J. E. M.), the National Science Foundation under Grant No. DMR-1918065 (A. A.), and a Simons Investigatorship (J. E. M.).

[*] These authors contributed equally.

[1] M. Z. Hasan and C. L. Kane, Colloquium: Topological insulators, Rev. Mod. Phys. **82**, 3045 (2010).
[2] V. P. Gusynin, S. G. Sharapov, and J. P. Carbotte, Unusual Microwave Response of Dirac Quasiparticles in Graphene, Phys. Rev. Lett. **96**, 256802 (2006).
[3] L. A. Falkovsky and A. A. Varlamov, Space-time dispersion of graphene conductivity, Eur. Phys. J. B **56**, 281 (2007).
[4] A. B. Kuzmenko, E. van Heumen, F. Carbone, and D. van der Marel, Universal Optical Conductance of Graphite, Phys. Rev. Lett. **100**, 117401 (2008).
[5] R. R. Nair, P. Blake, A. N. Grigorenko, K. S. Novoselov, T. J. Booth, T. Stauber, N. M. R. Peres, and A. K. Geim, Fine structure constant defines visual transparency of graphene, Science **320**, 1308 (2008).
[6] F. de Juan, A. G. Grushin, T. Morimoto, and J. Moore, Quantized circular photogalvanic effect in Weyl semimetals, Nat. Commun. **8**, 15995 (2017).
[7] M. Ezawa, Chiral anomaly enhancement and photoirradiation effects in multiband touching fermion systems, Phys. Rev. B **95**, 205201 (2017).
[8] Z.-M. Huang, J. Zhou, and S.-Q. Shen, Topological responses from chiral anomaly in multi-Weyl semimetals, Phys. Rev. B **96**, 085201 (2017).
[9] L. Lepori, M. Burrello, and E. Guadagnini, Axial anomaly in multi-Weyl and triple-point semimetals, J. High Energy Phys. 06 (2018) 110.
[10] F. Flicker, F. de Juan, B. Bradlyn, T. Morimoto, M. G. Vergniory, and A. G. Grushin, Chiral optical response of multifold fermions, Phys. Rev. B **98**, 155145 (2018).
[11] S. Rachel, Interacting topological insulators: A review, Rep. Prog. Phys. **81**, 116501 (2018).
[12] J. E. Avron and R. Seiler, Quantization of the Hall Conductance for General, Multiparticle Schrödinger Hamiltonians, Phys. Rev. Lett. **54**, 259 (1985).
[13] Q. Niu, D. J. Thouless, and Y.-S. Wu, Quantized Hall conductance as a topological invariant, Phys. Rev. B **31**, 3372 (1985).
[14] K. Ishikawa and T. Matsuyama, Magnetic field induced multi-component QED_3 and quantum Hall effect, Z. Phys. C **33**, 41 (1986).
[15] M. B. Hastings and S. Michalakis, Quantization of Hall conductance for interacting electrons on a torus, Commun. Math. Phys. **334**, 433 (2015).

[16] S. Coleman and B. Hill, No more corrections to the topological mass term in QED_3, Phys. Lett. **159B**, 184 (1985).
[17] A. Giuliani, I. Jauslin, V. Mastropietro, and M. Porta, Topological phase transitions and universality in the Haldane-Hubbard model, Phys. Rev. B **94**, 205139 (2016).
[18] A. Giuliani, V. Mastropietro, and M. Porta, Universality of the Hall conductivity in interacting electron systems, Commun. Math. Phys. **349**, 1107 (2017).
[19] R. B. Laughlin, Quantized Hall conductivity in two dimensions, Phys. Rev. B **23**, 5632 (1981).
[20] S. L. Adler, Axial-vector vertex in spinor electrodynamics, Phys. Rev. **177**, 2426 (1969).
[21] J. S. Bell and R. Jackiw, A PCAC puzzle: $\pi^0 \to \gamma\gamma$ in the σ-model, Nuovo Cimento A **60**, 47 (1969).
[22] S. L. Adler and W. A. Bardeen, Absence of higher-order corrections in the anomalous axial-vector divergence equation, Phys. Rev. **182**, 1517 (1969).
[23] A. Giuliani, V. Mastropietro, and M. Porta, Anomaly nonrenormalization in interacting Weyl semimetals, arXiv:1907.00682.
[24] A. A. Zyuzin and A. A. Burkov, Topological response in Weyl semimetals and the chiral anomaly, Phys. Rev. B **86**, 115133 (2012).
[25] A. A. Burkov, Chiral anomaly and transport in Weyl metals, J. Phys. Condens. Matter **27**, 113201 (2015).
[26] A. A. Burkov, Weyl metals, Annu. Rev. Condens. Matter Phys. **9**, 359 (2018).
[27] S. A. Parameswaran, T. Grover, D. A. Abanin, D. A. Pesin, and A. Vishwanath, Probing the Chiral Anomaly with Nonlocal Transport in Three-Dimensional Topological Semimetals, Phys. Rev. X **4**, 031035 (2014).
[28] S. Roy, M. Kolodrubetz, J. E. Moore, and A. G. Grushin, Chern numbers and chiral anomalies in Weyl butterflies, Phys. Rev. B **94**, 161107(R) (2016).
[29] C. Aversa and J. E. Sipe, Nonlinear optical susceptibilities of semiconductors: Results with a length-gauge analysis, Phys. Rev. B **52**, 14636 (1995).
[30] J. E. Sipe and A. I. Shkrebtii, Second-order optical response in semiconductors, Phys. Rev. B **61**, 5337 (2000).
[31] F. Nastos and J. E. Sipe, Optical rectification and current injection in unbiased semiconductors, Phys. Rev. B **82**, 235204 (2010).
[32] E. Deyo, L. E. Golub, E. L. Ivchenko, and B. Spivak, Semiclassical theory of the photogalvanic effect in noncentrosymmetric systems, arXiv:0904.1917.
[33] J. E. Moore and J. Orenstein, Confinement-Induced Berry Phase and Helicity-Dependent Photocurrents, Phys. Rev. Lett. **105**, 026805 (2010).
[34] E. J. König, H.-Y. Xie, D. A. Pesin, and A. Levchenko, Photogalvanic effect in Weyl semimetals, Phys. Rev. B **96**, 075123 (2017).
[35] L. E. Golub and E. L. Ivchenko, Circular and magneto-induced photocurrents in weyl semimetals, Phys. Rev. B **98**, 075305 (2018).
[36] T. Morimoto and N. Nagaosa, Topological nature of nonlinear optical effects in solids, Sci. Adv. **2**, e1501524 (2016).
[37] G. Chang, S.-Y. Xu, B. J. Wieder, D. S. Sanchez, S.-M. Huang, I. Belopolski, T.-R. Chang, S. Zhang, A. Bansil, H. Lin, and M. Z. Hasan, Unconventional Chiral Fermions and Large Topological Fermi Arcs in RhSi, Phys. Rev. Lett. **119**, 206401 (2017).
[38] D. Rees, K. Manna, B. Lu, T. Morimoto, H. Borrmann, C. Felser, J. E. Moore, D. H. Torchinsky, and J. Orenstein, Observation of topological photocurrents in the chiral Weyl semimetal RhSi, arXiv:1902.03230.
[39] G. E. Volovik, An analog of the quantum Hall effect in a superfluid ^{3}He film, JETP **67**, 1804 (1988), http://www.jetp.ac.ru/cgi-bin/e/index/e/67/9/p1804?a=list.
[40] V. Gurarie, Single-particle Green's functions and interacting topological insulators, Phys. Rev. B **83**, 085426 (2011).
[41] This is in contrast to the Coulomb interaction correction to the optical conductivity in Weyl semimetals, which was found to be universal [42].
[42] B. Roy and V. Juričić, Optical conductivity of an interacting weyl liquid in the collisionless regime, Phys. Rev. B **96**, 155117 (2017).
[43] I. F. Herbut, V. Juričić, and O. Vafek, Coulomb Interaction, Ripples, and the Minimal Conductivity of Graphene, Phys. Rev. Lett. **100**, 046403 (2008).
[44] V. Juričić, O. Vafek, and I. F. Herbut, Conductivity of interacting massless Dirac particles in graphene: Collisionless regime, Phys. Rev. B **82**, 235402 (2010).
[45] E. G. Mishchenko, Minimal conductivity in graphene: Interaction corrections and ultraviolet anomaly, Europhys. Lett. **83**, 17005 (2008).
[46] D. E. Sheehy and J. Schmalian, Optical transparency of graphene as determined by the fine-structure constant, Phys. Rev. B **80**, 193411 (2009).
[47] J. M. Link, P. P. Orth, D. E. Sheehy, and J. Schmalian, Universal collisionless transport of graphene, Phys. Rev. B **93**, 235447 (2016).
[48] I. Sodemann and M. M. Fogler, Interaction corrections to the polarization function of graphene, Phys. Rev. B **86**, 115408 (2012).
[49] B. Rosenstein, M. Lewkowicz, and T. Maniv, Chiral Anomaly and Strength of the Electron-Electron Interaction in Graphene, Phys. Rev. Lett. **110**, 066602 (2013).
[50] S. Teber and A. V. Kotikov, The method of uniqueness and the optical conductivity of graphene: New application of a powerful technique for multiloop calculations, Theor. Math. Phys. **190**, 446 (2017).
[51] S. Teber and A. V. Kotikov, Field theoretic renormalization study of interaction corrections to the universal ac conductivity of graphene, J. High Energy Phys. 82 (2018).
[52] D. Muñoz-Segovia and A. Cortijo, Many-body effects in nodal-line semimetals: Correction to the optical conductivity, arXiv:1910.08081.
[53] S. M. João and J. M. V. P. Lopes, Basis-independent spectral methods for non-linear optical response in arbitrary tight-binding models, J. Phys. Condens. Matter **32**, 125901 (2020).
[54] J. Rammer and H. Smith, Quantum field-theoretical methods in transport theory of metals, Rev. Mod. Phys. **58**, 323 (1986).
[55] D. E. Parker, T. Morimoto, J. Orenstein, and J. E. Moore, Diagrammatic approach to nonlinear optical response with application to Weyl semimetals, Phys. Rev. B **99**, 045121 (2019).

[56] H. Rostami and V. Juričić, Probing quantum criticality using nonlinear Hall effect in a metallic Dirac system, Phys. Rev. Research **2**, 013069 (2020).

[57] See Supplemental Material at http://link.aps.org/supplemental/10.1103/PhysRevLett.124.196603 for the details on the diagrammatic calculation of the CPGE coefficient and the interaction corrections to it, which also includes Ref. [58].

[58] M. E. Peskin and D. V. Schroeder, *An Introduction to Quantum Field Theory* (CRC Press, Boca Raton, 2018).

[59] The analytic continuation requires some extra care. Matsubara frequencies ω_1 and ω_2 must be taken either both positive or both negative. Otherwise, the real-frequency answer will be incorrect.

[60] M. Lv and S.-C. Zhang, Dielectric function, Friedel oscillation and plasmons in Weyl semimetals, Int. J. Mod. Phys. B **27**, 1350177 (2013).

[61] F. de Juan, Y. Zhang, T. Morimoto, Y. Sun, J. E. Moore, and A. G. Grushin, Difference frequency generation in topological semimetals, Phys. Rev. Research **2**, 012017 (2020).